

Reduced-dose patient to baseline CT rigid registration in 3D Radon space

Guy Medan, Achia Kronman, Leo Joskowicz

The Rachel and Selim Benin School of Computer Science and Engineering
The Hebrew University of Jerusalem, Israel
gmedan/leo.josko @mail.huji.ac.il

Abstract. We present a new method for rigid registration of CT scans in Radon space. The inputs are the two 3D Radon transforms of the CT scans to be registered, one densely sampled and the other sparsely sampled. The output is the rigid transformation that best matches them. The algorithm starts by finding the best matching between each direction vector in the sparse 3D Radon transform and the corresponding direction vector in the dense 3D Radon transform. It then solves the system of linear equations derived from the direction vector pairs. Our method can be used to register two CT scans and to register a baseline scan to the patient with reduced-dose scanning without compromising registration accuracy. Our preliminary simulation results on the Shepp-Logan head phantom dataset and a pair of clinical head CT scans indicates that our 3D Radon space rigid registration method performs significantly better than image-based registration for very few scan angles and comparably for densely-sampled scans.

1 Introduction

Rigid registration of CT scans acquired at different times plays a key role in numerous medical applications, including diagnosis, follow-ups, surgery planning and simulations. Rigid registration methods include intensity-based iterative registration methods, fiducial-based registration methods, and frequency-based registration methods. These methods are used routinely in a clinical environment and yield accurate results in most cases.

Rigid registration plays an increasingly important role in image-guided interventional CT procedures. Interventional CT procedures include biopsies, catheter insertion, hematoma evacuation, and many more. Often times, a high-quality CT scan of the patient is available before the procedure. Since the diagnosis and procedure planning is usually performed on this CT scan, it is desirable to use it for guidance during the intervention. In addition, repeated CT scanning is often performed during the intervention to evaluate anatomical changes and determine the location of surgical tools. This results in the exposure of the patient to ionizing radiation, which has been shown to have risks for the patient [1, 2]. It is thus highly desirable to develop methods that reduce the radiation dose required for intraoperative CT registration.

Two main approaches have been developed for rigid registration of CT scans: 1) image-based, and 2) Radon-based. Image-based methods, by far the most popular, perform the registration by comparing the intensity values of both scans. To yield adequate results, they require both CT scans to be of high quality and free of image reconstruction artifacts. Radon-space methods use the CT scans Radon transform representation (sinograms) for the registration. They are not subject to image reconstruction artifacts and have the potential to yield robust and accurate results with reduced-dose scanning.

Previous research addresses rigid registration in Radon space with a variety of methods. Freiman et al. [3] describe a method for 2D/3D registration of X-Ray to CT images. Their method uses invariant features in Fourier space to find the rigid parameters with out-of-plane coarse registration followed by in-plane fine registration. Mao et al. [4] describe a slice-by slice registration method in 2D Radon space and its extension to 3D/3D registration for small angles or with implanted fiducials, and Mooser et al. [5] use an iterative optimization process to find the registration parameters in 3D Radon space. You et al. [6] investigate the mathematical relation between rigid movement in image space and Radon space and its invariants, and in [7] Fourier phase matching technique is applied to this relation to allow recovery of the rigid registration parameters of translation and rotation using approximations for small angles. The parameters are extracted in a stage-by-stage manner that employs the result of the previous stage in the evaluation of the next parameters, by decomposing the 3D problem into a series of 2D in-plane registrations.

In this paper we describe a new method for rigid registration of CT scans in 3D Radon space. The inputs are the two 3D Radon transforms of the CT scans to be registered, one densely sampled and the other sparsely sampled. The output is the rigid transformation that best matches the 3D Radon transforms. The algorithm first finds for each direction vector in the sparse 3D Radon transform the best matching direction vector in the dense 3D Radon transform. It then constructs and solves a system of linear equations from the direction vector pairs. The advantages of our method are: 1) it can be used both to register two CT scans and to register a baseline scan to the patient with reduced-dose scanning without compromising registration accuracy; 2) it supports fast on-line patient to baseline CT scan registration; 3) it is robust to noise, small anatomical differences, and has a wide convergence range because it relies on a closed-form solution of a set of linear equations instead of an iterative process. Our preliminary simulation results on the Shepp-Logan head phantom dataset and a pair of clinical head CT scans indicate that our Radon space method performs significantly better than image-based registration for very few scan angles.

2 Method

We first present the mathematical background of the Radon transform and its application to CT scan rigid registration. We then describe our new 3D Radon space method and algorithm details.

Mathematical background. We follow the definitions and notations in [6] for parallel-beam scanning. Let $f : \mathfrak{R}^k \rightarrow \mathfrak{R}$ be an image function that maps k -dimensional location vectors to intensity values. Let $H(\mathbf{n}, s)$ be the hyperplane defined by normal direction vector \mathbf{n} and distance s from the origin in k -dimensional space. The Radon transform R of image function f is a function $Rf : S^{k-1} \times \mathfrak{R} \rightarrow \mathfrak{R}$ defined on unit sphere S^{k-1} of normal direction vector \mathbf{n} and distance s :

$$Rf(\mathbf{n}, s) = \int_{H(\mathbf{n}, s)} f(X) d\mu \quad (1)$$

where X is an k -dimensional vector and $d\mu$ is the standard measure on $H(\mathbf{n}, s)$. Let f, g be two image functions such that g is a similarity transformation of f :

$$g(X) = f(\rho A_{\mathbf{r}, \theta} X + X_0) \quad (2)$$

where $\rho > 0$ is the scaling constant, $X_0 \in \mathfrak{R}^k$ is the constant offset vector, and $A_{\mathbf{r}, \theta}$ is a unitary $k \times k$ matrix in which rotations are represented by an axis vector \mathbf{r} and an angle θ of rotation about \mathbf{r} . A well-known relation between the Radon transforms Rf, Rg of image functions f, g is:

$$Rg(\mathbf{n}, s) = \rho^{n-1} Rf(\mathbf{n}', \rho^{-1}(s + \mathbf{n} \cdot X_0)) \quad (3)$$

where \mathbf{n} and \mathbf{n}' are normal unit direction vectors satisfying:

$$\mathbf{n}' = A_{\mathbf{r}, \theta}^{-1} \mathbf{n} \quad (4)$$

This relation can be interpreted as follows. For a given normal unit direction vector \mathbf{n} , the Radon transforms of f and g , $Rf(\mathbf{n}, s)$ and $Rg(\mathbf{n}, s)$ are one-dimensional (1D) intensity signals of the distance s , which we denote by $F_{\mathbf{n}}(s) = Rf(\mathbf{n}, s)$ and $G_{\mathbf{n}}(s) = Rg(\mathbf{n}, s)$. Without offset and scaling, i.e. when $X_0 = \mathbf{0}$ and $\rho = 1$, Eq. 3 reduces to $Rg(\mathbf{n}, s) = Rf(\mathbf{n}', s)$, which means that the 1D signals $F_{\mathbf{n}'}(s)$ and $G_{\mathbf{n}}(s)$ are identical for direction vectors \mathbf{n} and \mathbf{n}' . That is, the projection in the direction \mathbf{n}' **before** the image f is rigidly rotated about the axis \mathbf{r} is **identical** to the projection in a different direction \mathbf{n} **after** the rotation, where the direction vectors \mathbf{n}, \mathbf{n}' are related by the same rotation $A_{\mathbf{r}, \theta}$. Furthermore, when the offset is not zero, that is $X_0 \neq \mathbf{0}$, we have:

$$G_{\mathbf{n}}(s) = F_{\mathbf{n}'}(s + \mathbf{n} \cdot X_0) \quad (5)$$

which means that $F_{\mathbf{n}'}(s)$ remains the same and is shifted by $\Delta = \mathbf{n} \cdot X_0$ for direction vectors \mathbf{n} and \mathbf{n}' .

In physical space, the image functions f, g are volumetric images; their Radon transform, $R_{3D}f, R_{3D}g$ are 3D, and the direction vectors are points on the unit sphere S^2 (Fig. 1). The spatial rigid transformation that relates f and g can be

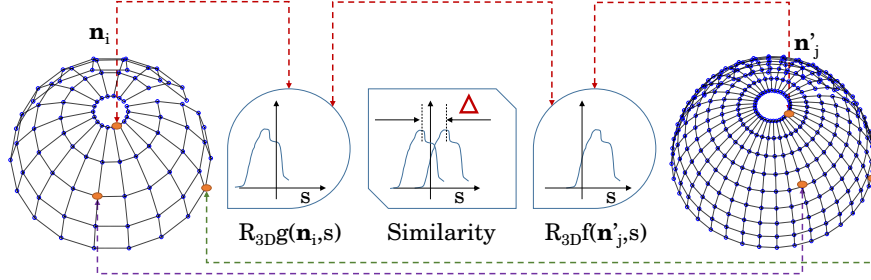


Fig. 1. Illustration of the matching procedure of 3D Radon transforms. $\mathbf{n}_i, \mathbf{n}'_j$ are direction vectors represented as points on the unit sphere. Each direction vector corresponds to a 1D projection signal $R_{3D}g(\mathbf{n}_i, s)$ or $R_{3D}f(\mathbf{n}'_j, s)$.

described by a translational offset X_0 , a rotation axis vector \mathbf{r} , and a rotation angle about it, θ . The goal of the rigid registration is to find the parameters $(\mathbf{r}, \theta, X_0)$ for which Eq. 2 holds.

The rigid transformation that aligns images f and g can be computed by matching their 3D Radon transforms, $R_{3D}f, R_{3D}g$, instead of matching the images themselves. This is called rigid registration in 3D Radon space. Furthermore, since Eq. 2 reduces to Eq. 5 without scaling, we can match $F_{\mathbf{n}'_j}(s)$ and $G_{\mathbf{n}_i}(s)$ where \mathbf{n}'_j and \mathbf{n}_i are the direction vectors of the 3D Radon transforms. When these Radon transforms are equal, that is when $G_{\mathbf{n}_i}(s) = F_{\mathbf{n}'_j}(s - \Delta_i)$ for offset Δ_i and direction vectors $\mathbf{n}_i, \mathbf{n}'_j$, then, from Eqs. 4 and 5 we get:

$$\Delta_i = \mathbf{n}_i \cdot X_0 \quad (6)$$

$$\mathbf{n}'_j = A_{\mathbf{r}, \theta}^{-1} \mathbf{n}_i \quad (7)$$

which is a set of linear equations. The desired rigid transformation parameters $(\mathbf{r}, \theta, X_0)$ can thus be computed by finding the pairs of direction vectors $\mathbf{n}_i, \mathbf{n}'_j$ that satisfy Eqs. 6 and 7. Three pairs of independent direction vectors suffice to fully determine the resulting linear system of equations.

In general, the similarity between $F_{\mathbf{n}'_j}$ and $G_{\mathbf{n}_i}$ does not imply Eqs. 6 and 7. Indeed, two identical 1D signals from two different direction vectors need not correspond to the same region of the images f and g ; this similarity may be coincidental. However, such coincidental signal matches are unlikely in CT scans of human anatomy, which is rich in complexity and detail, and is radially asymmetric. For most direction vector pairs, the matchings correspond to the same image region after rigid transformation. In addition, not all direction vector pairs yield rigid transformations within the expected range.

3D Radon rigid registration method. Based on these observations, we propose the following method for 3D Radon rigid registration of image g to

image f . The inputs are the 3D Radon transforms of g and f defined by direction vectors $\{\mathbf{n}_i\}_{i=1}^K$ and $\{\mathbf{n}'_j\}_{j=1}^L$. The goal is to build a set of matching projection pairs with relative displacements (Fig. 1).

For each direction vector \mathbf{n}_i we find the matching direction vector \mathbf{n}'_j and relative displacement Δ_i for which the corresponding 1D signals $G_{\mathbf{n}_i}$ and $F_{\mathbf{n}'_j}$ are most similar. The result is a set of matching pairs of projections, along with their relative displacements $\left\{ (F_{\mathbf{n}'_j}, G_{\mathbf{n}_i}, \Delta_i) \right\}_{i=1}^K$.

Substituting each direction vector pair in Eqs. 6 and 7 yields an overdetermined set of linear equations. We compute the desired rigid transformation parameters $(\mathbf{r}, \theta, X_0)$ by least-squares minimization. Offset X_0 is estimated as $\hat{X}_0 = (\mathbf{N}^T \mathbf{N})^{-1} \mathbf{N}^T \mathbf{\Delta}$ where $\mathbf{N} = [\mathbf{n}_1 \dots \mathbf{n}_K]^T$ and $\mathbf{\Delta} = [\Delta_1 \dots \Delta_K]^T$. This solution minimizes the term $\sum_{i=1}^K (\Delta_i - \mathbf{n}_i \cdot X_0)^2$.

To estimate the rotation matrix $A_{\mathbf{r}, \theta}$, we define the 3×3 matrix $M = \sum_{i=1}^K \mathbf{n}'_{j(i)} \mathbf{n}_i^T$ and compute its Singular Value Decomposition $M = U^T \Sigma V$. From the values of U, V we obtain the estimate $\hat{A}_{\mathbf{r}, \theta} = UV^T$. This solution minimizes the term $\sum_{i=1}^K (\mathbf{n}_i - A_{\mathbf{r}, \theta} \mathbf{n}'_{j(i)})^2$.

A key property of this method is that it does not require a dense set of direction vectors of the 3D Radon transform of image g . Since the set of linear equations from which the transformation parameters are computed is of dimension 3, the set is overconstrained with more than three direction pairings. Using more direction pairs that are not outliers usually increases robustness and improves accuracy. This is akin to point-based rigid registration, in which more than three point pairs are used. The method is therefore suitable for finding the rigid registration between sparsely and densely sampled set of direction vectors for $R_{3D}g$ and $R_{3D}f$. This is the situation of interventional CT procedures that require registering the patient with his/her earlier CT scan.

3D Radon rigid registration algorithm. We now describe a new 3D Radon rigid registration algorithm based on the method described above. The inputs are the two Radon transforms $R_{3D}f$ and $R_{3D}g$ of images f and g . The output is the rigid transformation $(\mathbf{r}, \theta, X_0)$. The algorithm consists of two steps. First, for each direction vector in the sparse $R_{3D}g$ transform, we find the matching direction vector in the dense $R_{3D}f$ transform. Then, we construct and solve the set of linear equations obtained by substituting each direction vector pair in Eqs. 6 and 7. We describe each step in detail next.

1. Direction vectors pairing. We evaluate the similarity of the two 1D signals from two direction vectors with Normalized Cross Correlation (NCC); the NCC value is the direction vectors pair score. For each direction vector \mathbf{n}_i , we select the direction vector \mathbf{n}'_j with the highest NCC score and compute its relative displacement Δ_i . We define an index function $match(i) = argmax_j \{NCC(R_{3D}g(\mathbf{n}_i, s), R_{3D}f(\mathbf{n}'_j, s))\}$ that pairs the direction vectors. To avoid searching all possible direction vectors \mathbf{n}'_j , we restrict the search to a neighbourhood of \mathbf{n}_i defined by $\Phi(\mathbf{n}_i) = \{\mathbf{n}'_j : \cos^{-1}(\mathbf{n}_i \cdot \mathbf{n}'_j) < \varphi\}$ where φ is the largest expected relative orientation offset between the images.

2. *Transformation computation.* We construct and solve the set of linear equations obtained by substituting each direction vector pair in Eqs. 6 and 7 as described above. We use RANSAC to eliminate outliers. Since the resulting set of equations is 3-dimensional, we obtain high-quality results with a large number of RANSAC iterations in a short time. We set the RANSAC inliers threshold ψ for the relative angle $\cos^{-1}(\mathbf{n}_i^T \hat{A}_{r,\theta} \mathbf{n}'_j)$ to be half the angular resolution of the densely-sampled set $R_{3D}f$.

Computation of 3D Radon transforms from 2D sinograms. The 3D Radon transform $R_{3D}g$ of the baseline image f can be efficiently computed from the 2D sinograms of the slices as described in [5]. Our algorithm achieves the desired rigid registration with a sparse sampling of $R_{3D}g$, which takes place in the CT scanner. The reduced number of direction vectors required thus leads to a significant reduction of the radiation dose without compromising accuracy and without having to reconstruct the image g .

3 Experimental results

To evaluate our method, we conducted the following simulation experiments in Matlab. We use the Shepp-Logan head phantom dataset whose size is $256 \times 256 \times 256$ voxels with intensity values in $[0, 1]$. To simulate data acquisition noise, we add $N(0, 0.05)$ Gaussian noise to the dataset to obtain the baseline image f . We then apply to f a series of rigid transformation including both rotations and translations to generate a new set of images h (Table 1). For each image h , we generate its sinograms by projection and create a set of new sparsely-sampled images $\{g_l\}$. Each image g_l is created by filtered back projection from 2 to 18 projection directions instead of the usual 180 required for full-resolution reconstruction. The resulting images include significant reconstruction artifacts.

Parameter Setting	Axis vector \hat{r} <i>not normalized</i>	Angle θ <i>degrees</i>	Translation X_0 <i>pixels</i>
1	(1, 2, 100)	1.0	(2, 0, -1)
2	(34, 45, 39)	-7.7	(14, 15.2, -18.5)
3	(23, -12, 1)	13.2	

Table 1. Parameters and settings for the ground-truth transformations. A total of 18 rigid transformations (all possible $3 \times 3 \times 2$ possible combinations).

We then perform two sets of rigid registrations: one in image space using Matlab’s `imregtform` and the other one in Radon space with our method. In image space, we compute the rigid transformation parameters between the original phantom image f and the reconstructed and transformed phantom images g_l . In Radon space we applied our registration method on the 3D Radon transforms of f and g_l . The 3D Radon transform of f was computed at an angular resolution of 1° for 180 2D projection directions per slice, for a total of 32,400 direction vectors. The resulting rigid transformations of the image-based and Radon-based

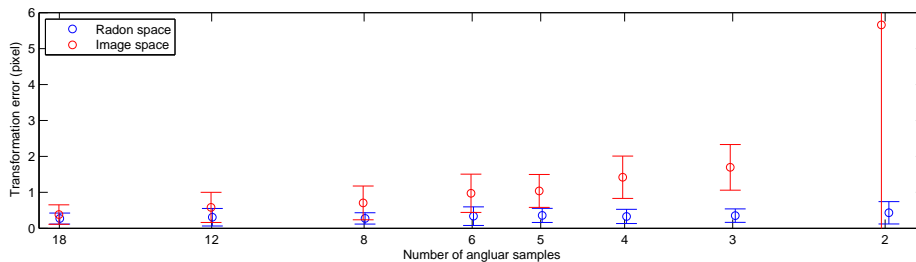


Fig. 2. Plot of the image-based (red) and 3D Radon (blue) rigid transformation error with respect to the ground-truth transformation (vertical axis) as a function of the number of scan angles (horizontal axis), 18 to 2.

registration were then applied to the original image f . The resulting images were compared to the ground-truth rigid transformations of f by computing the RMS error between 3D voxel coordinates. The experiment was repeated between 3 to 10 times for each rigid transformations and sparse sampling settings. Fig. 2 shows the results. Note that our Radon space method performs significantly better than image-based registration for very few scan angles (< 12). Note also that our algorithm handles well rotation offsets $> 10^\circ$, which are challenging for other algorithms that rely on small-angle approximations.

In a second experiment, we test our method on a pair of CT scans from a patient head taken at two different times. The voxel sizes of the CT scans are $0.42 \times 0.42 \times 0.67 \text{ mm}^3$. Prior to registration, we removed the scanning bed from both images, as the bed is not rigidly attached to the patient and introduces errors in the Radon space signals. In practice, this can be done automatically, since the Radon transform of the bed without the patient is always the same and can be precomputed and subtracted from the patient scan. We then computed the image-based registration of the full-resolution scans and our Radon space registration with the second image from 18 angles using our method and compared the results (Fig. 3). The RMSE between the image space registration and our method is 0.64mm. This indicates that our method yields results comparable to full-resolution image-space registration with about 10% of the radiation dose of the second scan.

4 Conclusions

We have presented a new 3D Radon space rigid registration method for CT scans registration. Our method can be used to register two existing CT scans and to register a baseline CT scan to the patient for interventional CT procedures. The key characteristic of our method is that it allows the registration of a full-resolution CT scan to a sparsely-sampled CT scan without compromising the registration accuracy. This results in a significant X-ray dose reduction when registering a diagnostic CT scan to the patient prior to image-guided interventional CT procedures. Another advantage of our method is that it supports fast

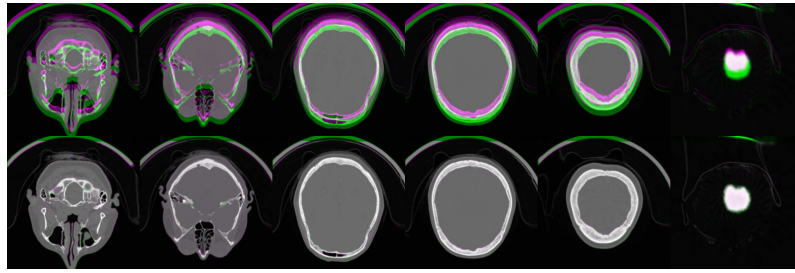


Fig. 3. Overlay of six representative slices from two head CT scans of the same patient: before registration (top row), after 3D Radon space registration (bottom row).

on-line patient to baseline CT scan registration, as most of the 3D Radon space computation on the baseline image can be performed prior to the intervention. Our preliminary results indicate that a very small number of scan directions are sufficient to obtain voxel size accuracy, that the method has a wide convergence range, and that it is robust to small anatomical differences.

Future work includes extending our formulation of parallel-beam CT acquisition to cone beam and spiral acquisition, conducting more extensive simulation experiments, and conducting studies with actual CT sinograms.

References

1. Chodick, G., Ronckers, C.M., Shalev, V., Ron, E., et al.: Excess lifetime cancer mortality risk attributable to radiation exposure from computed tomography examinations in children. *IMAJ-RAMAT GAN*- **9**(8) (2007) 584.
2. Mettler Jr, F.A., Wiest, P.W., Locken, J.A., Kelsey, C.A.: CT scanning: patterns of use and dose. *Journal of Radiological Protection* **20**(4) (2000) 353.
3. Freiman, M., Pele, O., Hurvitz, A., Werman, M., Joskowicz, L.: Spectral-based 2d/3d X-ray to CT image rigid registration. In: *SPIE Medical Imaging, International Society for Optics and Photonics* (2011) 79641B–79641B.
4. Mao, W., Li, T., Wink, N., Xing, L.: CT image registration in sinogram space. *Medical physics* **34**(9) (2007) 3596–3602.
5. Mooser, R., Forsberg, F., Hack, E., Székely, G., Sennhauser, U.: Estimation of affine transformations directly from tomographic projections in two and three dimensions. *Machine vision and applications* **24**(2) (2013) 419–434.
6. You, J., Lu, W., Li, J., Gindi, G., Liang, Z.: Image matching for translation, rotation and uniform scaling by the radon transform. In: *Image Processing, 1998. ICIP 98. Proceedings. 1998 International Conference on. Volume 1., IEEE* (1998) 847–851.
7. Lu, W., Fitchard, E.E., Olivera, G.H., You, J., Ruchala, K.J., Aldridge, J.S., Mackie, T.R.: Image/patient registration from (partial) projection data by the fourier phase matching method. *Physics in Medicine and Biology* **44**(8) (1999) 2029.